Fuel Economy Benefits of Electrified Powertrains with Advanced Combustion Engines: Mild to Strong HEV Applications

Ali Solouk[1], Mahdi Shahbakhti[2]

1: Ford Motor Company, 21500 Oakwood Blvd., Dearborn, MI 48124 USA
2: Michigan Technological University, 1400 Townsend Dr., Houghton, MI 49931 USA

Abstract: Powertrain electrification including hybridizing advanced combustion engines is a viable cost-effective solution to improve fuel economy of vehicles. This will provide opportunity for narrow-range high-efficiency combustion regimes to be able to operate and consequently improve vehicle's fuel conversion efficiency, compared to conventional hybrid electric vehicles. Low temperature combustion (LTC) engines offer the highest peak brake thermal efficiency reported in literature, but these engines have narrow operating range. In addition, LTC engines have ultra-low soot and NOx emissions, compared to conventional compression ignition and spark ignition (SI) engines. In this study, advanced easily verifiable optimal control techniques are employed as the energy management supervisory controller to investigate hybridization of multi-mode LTC-SI engines for applications ranging from mild to strong hybrid electric vehicles (HEVs).

A multi-mode LTC-SI engine is experimentally developed at Michigan Tech. University and the engine operating modes include homogeneous charge compression ignition (HCCI), reactivity controlled compression ignition (RCCI), and conventional SI. The powertrain controller is designed to enable switching among different modes, with minimum fuel penalty for transient engine operations. Moreover, the engine emissions are controlled by considering the catalytic convertor light-off temperature in the control framework for selecting the engine operating points. The developed multi-mode engine is analysed in series architecture and P2 parallel architecture in various hybridization levels.

Keywords: High Efficiency Engines, Low Temperature Combustion, Hybrid electric vehicles, Optimal Energy Management

1. Introduction

The U.S. light-duty (LD) vehicle regulations require a fleet average of 4.3 liter/100 km fuel consumption by 2025 to meet the 101 g/km CO2 regulation [1]. In the E.U. new vehicles must meet an average fleet fuel consumption of 4.1 liter/100 km by 2021 [2]. High efficiency engines coupled with powertrain electrification will play a critical role in meeting these upcoming stringent requirements [3, 4, 5]. Manufacturers in the U.S. currently prefer spark-ignition (SI) engines fuelled with gasoline to other types of combustion engines [1]. On the other hand, conventional compression ignition (CI) engines are noteworthy for the LD vehicles due to their high brake thermal efficiency. However, CI engines require an expensive and complex aftertreatment system for particular matter (PM) and NOx control [6]. There is a need for technology that improves fuel consumption and circumvents the emissions problem.

Various studies have investigated advanced combustion regimes to address this need [7, 8, 9]. One promising advanced combustion regime is low temperature combustion (LTC); LTC consists of a family of variants including homogeneous charge compression ignition (HCCI), reactivity controlled compression ignition (RCCI), and partially premixed compression ignition (PPCI) [10, 11]. LTC engines offer a peak indicated thermal efficiency of 53% with much lower NOx and PM engine-out emissions than traditional CI engines [9, 12]. The gains in thermal efficiency and the cost reduction of the aftertreatment system are offset, in part, by two challenges: LTC engines have narrow operating ranges and they require more complex combustion control [13]. To mitigate the impact of these challenges, this paper investigates the integration of a single-mode and multi-mode LTC engine in electrified powertrains including series and parallel. In the series architecture, decoupling of the ICE from the drivetrain allows the LTC engine to operate in its narrow high-efficiency combustion regime while significantly reducing the complexity of the engine combustion control needed during mode transitions. Moreover, in the parallel architecture, the e-motor torque assist allows to keep the engine in the LTC narrow-range high-efficiency combustion regime and reduce the required number of mode-switching to the conventional SI mode.

This works builds upon our previous studies in references [14] and [15]. The investigation in this paper considers experimental mode switching fuel penalty maps, NVH constraints, and the exhaust gas temperature constraint according to exhaust aftertreatment light-off temperature. Thus, the optimization results in this work are more realistic, compared to our previous studies in [14] and [15].

2. Multi-Mode LTC-SI Engine and Electric Powertrain Experimental Setup

This section introduces the experimental setup for this study, which enables the investigation of different aspects of HEV powertrains with an LTC-SI engine. The experimental setup was designed and constructed at Michigan Technological University and is shown in Figure 1. The setup is comprised of a fuel-flexible 2.0-liter LTC-SI engine and a 100-kW electric powertrain, which are connected to a 465 hp AC dynamometer. The LTC-SI engine can operate in the HCCI and RCCI modes and also in conventional SI mode. The electric powertrain setup is capable of simulating the HEV powertrain during different loads and speeds. The experimental setup is equipped with a proper control platform to implement energy management strategies. Details of the experimental setup are found in references [14] and [15].

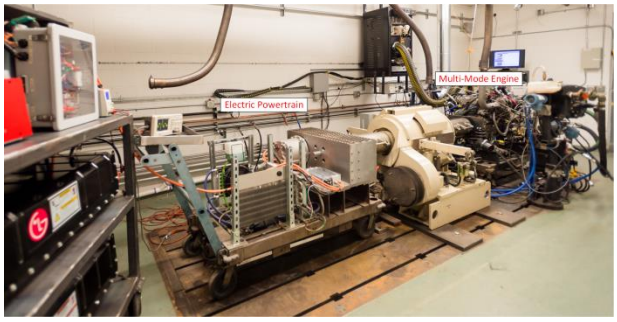

Figure 1: Developed LTC-based hybrid electric powertrain experimental testbed with a double- ended 465 hp AC dynamometer at Michigan Technological University.

2.1. Engine Experimental Maps

Using the data acquired from dSPACE®, LabVIEW® and ACAP®, the combustion and performance parameters were calculated using an in-house Matlab® code. The brake specific fuel consumption (BSFC) maps were generated and the load limits for each of the combustion modes were determined. Figure 2 shows the BSFC maps for the SI, HCCI and RCCI combustion modes with engine speed (RPM) on the x-axis and power (kW) on the y-axis. As can be seen in Figure 2, the HCCI engine has a limited operating range in comparison to the SI engine. The HCCI engine maximum power is 14 kW, compared to 25 kW and 50 kW for the RCCI and SI engines, respectively, for the test conditions in this study. Further, the HCCI and SI engines are at the two opposite ends of the spectrum with highest and lowest available maximum Brake Thermal Efficiency (BTE) i.e., minimum BSFC.

The measured exhaust gas temperatures are shown in Figure 3 for the SI, RCCI, and HCCI operating modes. The SI engine exhaust gas temperature ranges from 457°C to 776 °C. This temperature range changes to 246–660 °C, and 200–442 °C for the RCCI and HCCI operating modes, respectively. The engine operating points are selected to meet the minimum catalyst light-off temperature (i.e., 300 °C [16]) such that emissions standards are met. This is implemented by considering the engine exhaust gas temperature as a constraint in the optimization framework, which will be discussed in Section 3.

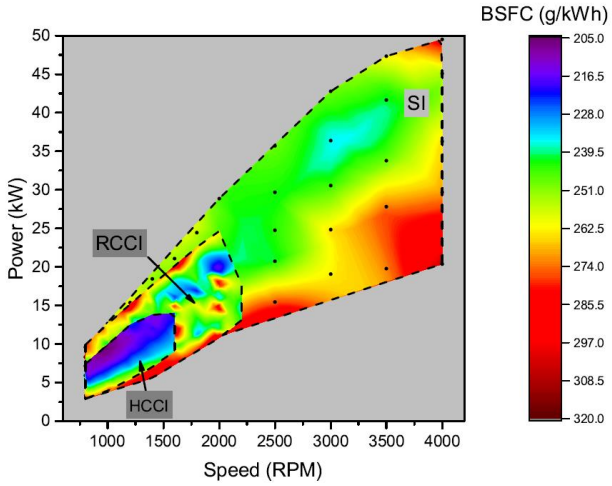

Figure 2: Experimental BSFC map of the developed multi-mode LTC-SI engine. Data points are shown by dot symbols.

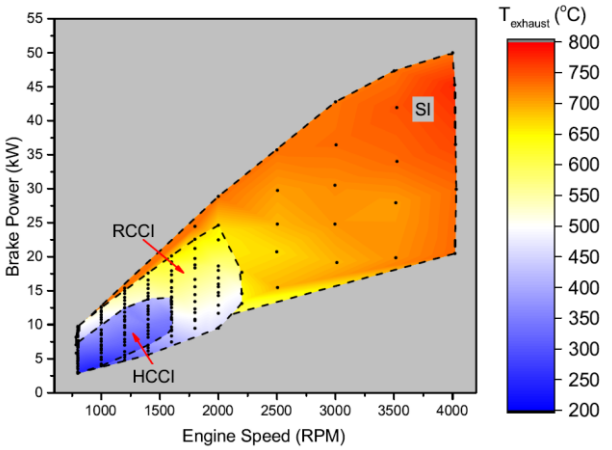

Figure 3: Experimental exhaust gas temperature map of the developed multi-mode LTC-SI engine. Data points are shown by dot symbols.

The engine can operate in the HCCI, RCCI, and SI modes. Mode switching strategies were developed to leverage the selection of engine mode in energy management strategy. Under small road loads, the vehicle should take advantage of the higher thermal efficiency of the LTC modes. As road load increases, the vehicle should switch to the SI mode - either because it is more efficient or because the LTC modes are incapable of meeting the road load. The fuel penalty for switching modes is an important

component of the switching strategy. The fuel penalty for switching from RCCI to SI and SI to HCCI were determined experimentally [17]. All other mode switches do not include a fuel penalty. Figure 4 highlights the fuel penalty map for switching from SI to HCCI and RCCI to SI for different engine speeds and torques.

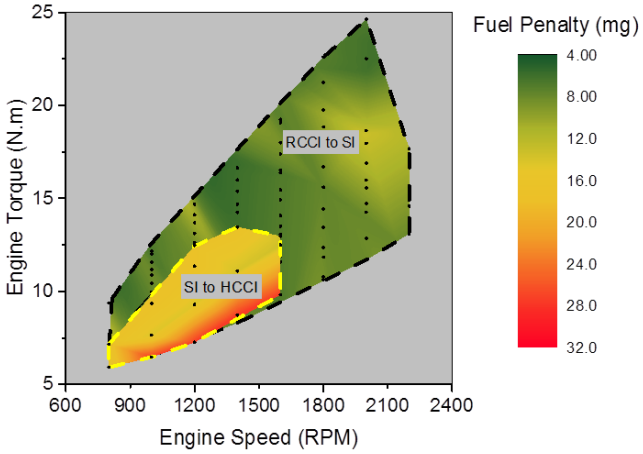

Figure 4: Experimental mode-switching fuel penalty map.

2.2. Electric Powertrain Data

Figure 5 shows the e-motor efficiency map that is experimentally calculated using the data in this study by testing the e-motor at a range of speeds and torques. The data is collected at the e-motor temperature of 45°C and the DC voltage of 360 V. Under these conditions, the e-motor efficiency ranges from 71.7 to 91.2 percent. In the next section, the designed optimal energy management strategy is presented. The optimal strategy is implemented for the series and parallel HEV models with the experimentally validated components.

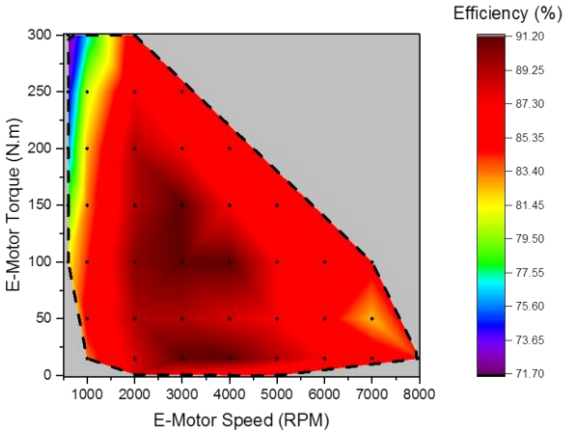

Figure 5: Combined calculated efficiency map including efficiency of the synchronous PMSM Remy motor and transaxle mechanical losses. Test conditions: e-motor temperature=45 °C and DC bus voltage=360 V.

3. Design of Optimal Control for the Multi-Mode LTC-SI in Electrified Powertrain

The goal of the optimal control in this study is to minimize the fuel consumption ($\dot{m}_f$) during the time that the range extender is active. The cost function under the optimization is defined by Eq. (1):

$$J(u(t)) = \int_0^T \dot{m}_f \, dt \qquad (1)$$

where $\dot{m}_f$ is the rate of the engine fuel consumption and T is the time length of a driving cycle. Equation (2) shows the constraints for the HEV optimization problem.

$$|SOC_f - SOC_0| \leq 0.01 \qquad (2\text{-a})$$
$$SOC_{min} \leq SOC(t) \leq SOC_{max} \qquad (2\text{-b})$$
$$P_{bat,min} \leq P_{bat}(t) \leq P_{bat,max} \qquad (2\text{-c})$$
$$P_{eng,min}(\omega_{eng}) \leq P_{eng}(t, \omega_{eng}) \leq P_{eng,max}(\omega_{eng}) \qquad (2\text{-d})$$
$$\omega_{eng,min} \leq \omega_{eng}(t) \leq \omega_{eng,max} \qquad (2\text{-e})$$
$$P_{mot,min}(\omega_{mot}) \leq P_{mot}(t) \leq P_{mot,max}(\omega_{mot}) \qquad (2\text{-f})$$
$$\omega_{mot,\min} \leq \omega_{mot}(t) \leq \omega_{mot,max} \qquad (2\text{-g})$$
$$Temp_{exh}\ (\omega_{eng}, T_{eng} \geq Temp_{\,light-off} \qquad (2\text{-h})$$

The constraints in the optimization framework include the battery SOC operation window, battery power (P_{bat}), engine power (P_{eng}), engine speed (ω_{eng}), e-motor power (P_{motor}), e-motor speed (ω_{motor}), and oxidation catalyst light-off temperature ($Temp_{light-off}$) in the exhaust aftertreatment system. The controller selects the engine operating regions where the exhaust gas temperature is greater than the catalytic converter light-off temperature (i.e., 300 °C [16]) to achieve low tailpipe HC and CO emissions. NOx and soot emissions are ultra-low in LTC modes [10]. In addition, a NVH constraint is included to avoid running the engine at low speed when vehicle speed is low:

$$\omega_{eng} \leq 1500\, rpm, \quad if\ V_{veh} \leq 40\ {}^{km}/_{h} \qquad (3)$$

The PMP optimal control solution is used for the analysis in this work. A constraint of maximum one percent ΔSOC variation is considered for the charge-sustaining mode. The optimal control problem is solved using PMP and the battery SOC is in the charge-sustaining mode.

3.1. Pontryagin's Minimum Principal (PMP)

The PMP method is based on a general case of the Euler-Lagrange equation and originates from the Calculus of Variation. It yields the necessary -not sufficient conditions of the optimal solution. In this framework, an optimal solution is any unique trajectory that meets the necessary conditions for optimality and also meets the boundary conditions for the problem being solved. Before addressing conditions for optimality, the pseudo-dynamic model

of the vehicle and a technique to determine the Hamiltonian values of that model are introduced.

3.2. Vehicle Models

Figure 6 shows the series and parallel vehicle architectures equipped with the multi-mode LTC-SI engine.

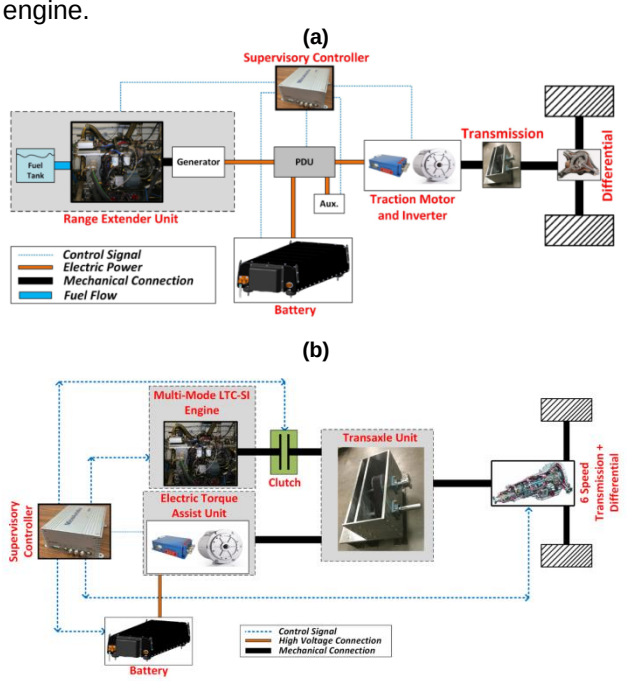

Figure 7: Series and parallel HEV architecture in this study. PDU stands for power distribution unit.

In the P2 parallel HEV architecture, the engine is coupled to the e-motor through a clutch. The output shaft is connected to the drivetrain where an automatic six speed transmission connects the output shaft to the wheels. This limits the engine operating points to discrete gear ratio options. The operating maps and model parameters for the vehicle components are obtained from the experimental setup as explained in the Section 2. Details of vehicle models are found in [14] and [15].

4. Optimization Results

In this section optimization results for the LTC-SI engine in series and parallel HEV architectures are discussed. In the first subsection, the results for series architecture with both dedicated single-mode engine including HCCI, RCCI, SI, and multi-mode LTC-SI engines are presented. In the next subsection, the results for the multi-mode LTC-SI in parallel P2 architecture are explained. It should be noted that the battery is in charge-sustaining mode in this study to have a meaningful fuel consumption comparison. The series architecture results in this work are mainly based on [14], but the exhaust gas temperature and NVH constraints and experimental mode-switching fuel penalty map are added to the results presented in this work. Moreover, in the P2 parallel architecture, compared to the results presented in [15], the exhaust gas temperature constraint and the experimental mode-switching fuel penalty are included in this work plus a small sedan is considered as a baseline vehicle for the simulations.

4.1 Series HEV

The main goal of charging-path optimization is to make the engine and generator operate at their optimum efficiency points by taking into account the exhaust gas temperature and NVH constraints defined in Equations (2-h) and (3). The operating points of the discharging-path, on the other hand, are dictated by the road load and vehicle design parameters. The costate in the PMP is selected such that the SOC is balanced at the end of the driving cycle. For each cycle, depending on available negative power at the wheels, the PMP methodology optimizes the system operating points such that the battery SOC stays as close as possible to the SOC in which the battery has the lowest internal resistance (R). In fact, the dependency of battery resistance and voltage on SOC makes the charging-path optimization linked to the driving cycle.

Figure 8 shows the fuel consumption improvement of the multi-mode LTC-SI and the single-mode LTC range extenders over the single-mode SI engine in the series architecture. It illustrates that the highest fuel consumption reduction is achieved in the multi-mode case with 12.4% reduction in fuel consumption in the UDDS which is 1.4% higher than the best single-mode achieved fuel consumption (i.e., HCCI engine). The multi-mode engine offers the lowest fuel consumption for driving cycles that result in greater difference between the HCCI and RCCI engines BTE and engine ON time values. On the other hand, for HWFET driving cycle where both RCCI and HCCI engines have close engine BTE and ON time values, the multi-mode engine does not provide higher fuel consumption benefit. In fact, in that case the fuel consumption is slightly higher compared to the single-mode HCCI due to the mode-switching fuel penalty.

Figure 9 shows the engine operating points of the multi-mode engine for the three driving cycles. As the figure shows the engine does not operate in the SI mode for the UDDS and HWFET driving cycles. However, in the US06 driving cycle the engine switches to the SI mode for a short amount of time (See Figure 9). This behavior can be explained by comparison of the average wheel power demand of the three driving cycles. Due to higher engine efficiency in the HCCI compared to the RCCI and SI modes, the ideal case is to let the engine operate in the efficient HCCI mode for the lower power demand

driving cycles. However, for cases that the driving cycle's average and instantaneous powers are high (i.e., US06), the engine tends to operate mostly in the RCCI and SI modes.

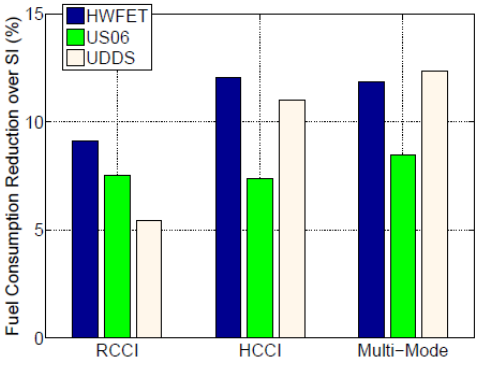

Figure 8: Fuel consumption reduction of the series HEV running with different engines over the SI engine during UDDS, HWFET, and US06 driving cycles.

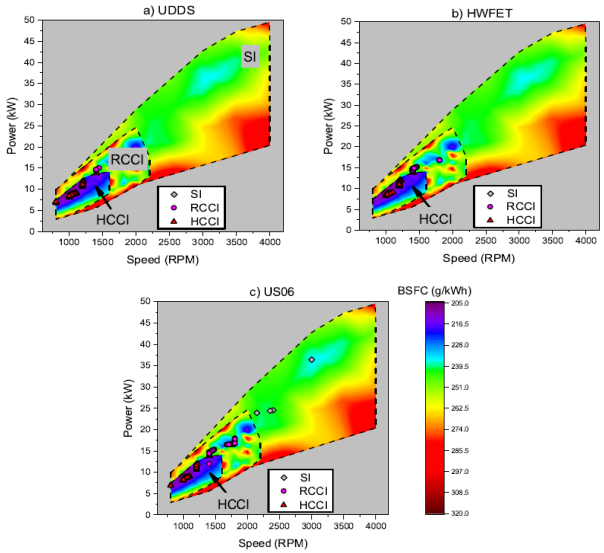

Figure 9: Engine operating points over the multi-mode engine BSFC maps in series HEV architecture for UDDS, HWFET, and US06 driving cycles.

4.2 Parallel P2 HEV

The PMP approach is utilized to investigate potential energy saving in the multi-mode LTC-SI engine in the parallel HEV configuration. Three different levels of hybridization are defined by the P_{bat}/P_{eng} ratio, as listed in Table 1.

Table 1: Definition of hybridization levels for the P2 architecture in this study

Hybridization	$\frac{P_{batt}}{P_{eng}}$	Electric Motor Power (kW)	Operating Voltage (V)
PHEV	1.0	60	270-410
Full Hybrid	0.65	40	180-270
Mild Hybrid	0.30	18	80-120

PHEV has the highest electrification level with peak 60 kW e-motor power and peak 410 V battery voltage. The battery and e-motor power limit in the full hybrid category is defined as 40 kW; this number reduces to 18 kW for the mild hybrid. Figure 10 shows the single-mode SI engine BSFC map along with the engine operating points at two hybridization levels.

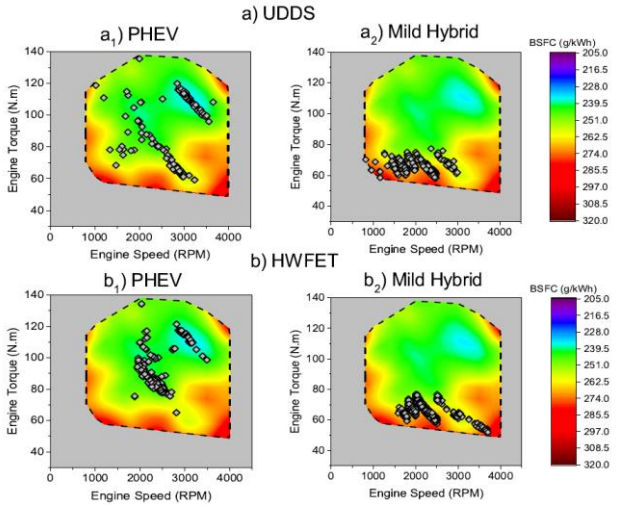

Figure 10: Engine operating points over the single-mode engine BSFC map for different electrification levels in the parallel HEV during a) UDDS and b) HWFET driving cycles.

The engine optimum operating points are shown for the UDDS and HWFET driving cycles. In both UDDS and HWFET driving cycles, the high power engine operating points are located in the low BSFC region (i.e., BSFC < 240 g/kWh) for the PHEV, while the engine operating points shift to the low torque and high BSFC regions (i.e., BSFC > 260 g/kWh) when the hybridization level decreases to mild hybrid category. In addition, in the mild hybrid, the engine operating points are more dependent on wheel speed and power demand since the e-motor assist torque is more limited. This results in less flexibility for the torque management controller to place the engine operating points to the low BSFC region. However, a higher battery and e-motor power in the PHEV provides more flexibility for the hybrid powertrain to shift the engine operating points to the more efficient engine regions, while maintaining the battery SOC. Hence, the engine ON time, as listed in

Table 2, reduces to 184 sec in PHEV compared to 385 sec in mild hybrid for the UDDS. In the HWFET driving cycle, as listed in Table 3, the engine ON time reduces from 1052 sec to 739 sec by moving from mild hybrid to PHEV.

Table 2: Parallel HEV results for both multi-mode LTC-SI and single-mode SI engine in different electrification levels during UDDS driving cycle

Metrics	Multi-Mode LTC-SI			Single-Mode SI		
	PHEV	Full HEV	Mild HEV	PHEV	Full HEV	Mild HEV
Fuel consumption(g)	356.3	344.5	378.9	365.5	358.2	409.8
CO2 emissions (g)	1000.2	967.1	1063.8	1026.1	996.5	1120.0
Ave. engine BTE (%)	34.0	34.3	33.0	33.0	33.6	31.4
Engine work(MJ)	4.80	4.67	5.01	4.90	4.90	5.05
Engine ON time (sec)	233	259	451	184	198	385
Battery loss (kJ)	582.3	396.8	307.1	622.6	452.0	351.6

Table 3: Parallel HEV results for both multi-mode LTC-SI and single-mode SI engine in different electrification levels during HWFET driving cycle

Metrics	Multi-Mode LTC-SI			Single-Mode SI		
	PHEV	Full HEV	Mild HEV	PHEV	Full HEV	Mild HEV
Fuel consumption(g)	1168.0	1184.3	1207.2	1170.2	1192.9	1216.0
CO2 emissions (g)	3324.1	3417.7	3516.8	3361.5	3442.7	3542.4
Ave. engine BTE (%)	34.5	34.2	31.7	34.2	34.1	31.4
Engine work(MJ)	16.1	16.4	15.6	16.2	16.5	15.7
Engine ON time (sec)	850	818	1084	739	798	1052
Battery loss (kJ)	785.3	716.6	431.6	792.1	769.8	519.0

Figure 11 shows the multi-mode LTC-SI engine BSFC map and the engine operating points over the UDDS and HWFET driving cycles. The engine operating points are illustrated for both PHEV and mild hybrid. Figure 11-a2 shows that the high BSFC operating points are running in the LTC modes (i.e., RCCI, HCCI) in the multi-mode engine. Increasing the running time of LTC modes reduces the overall fuel consumption of the vehicle. LTC modes benefit fuel economy in the mild hybrid vehicle over city driving cycle (i.e., UDDS) the most, since it increases the engine brake thermal efficiency (BTE) without charging the battery. In the PHEV, however, the multi-mode LTC-SI engine has less advantage compared to the mild HEV due to availability of higher electric power for locating the engine operating points in high power SI regions with less engine ON time (see Table 2 and Table 3). Moreover, in Figure 11-a2 the engine operates in SI mode over the low engine speeds (i.e., 800 – 1600 rpm) and mid engine torques (i.e., 60 – 80 N.m), while the engine could operate in HCCI mode with a lower BSFC. The optimizer decided to keep the engine on the SI mode in that region due to higher SI-HCCI mode-switching fuel penalty (see Figure 4).

The vehicle fuel consumption is shown in Figure 12 for both UDDS and HWFET driving cycles. The results show the advantage of the multi-mode LTC-SI engine in the mild hybrid over the single-mode SI. However, this improvement rate is smaller over the HWFET driving cycle since the engine operating points are located mainly in fuel-efficient regions independent of the electrification level.

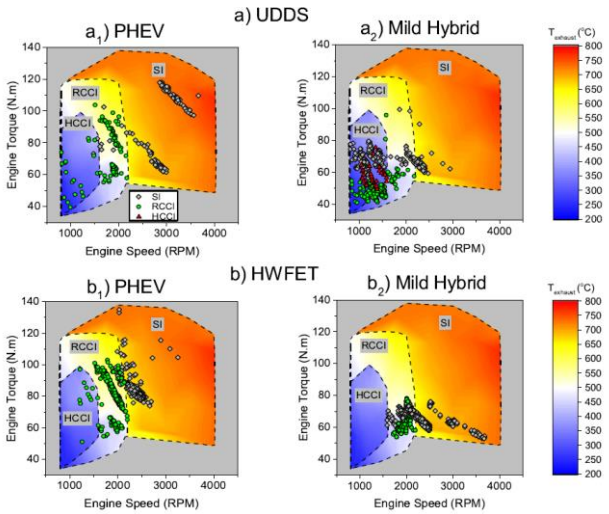

Figure 11: Engine operating points over the multi-mode engine BSFC map for different electrification levels in the parallel HEV architecture for a) UDDS and b) HWFET driving cycles.

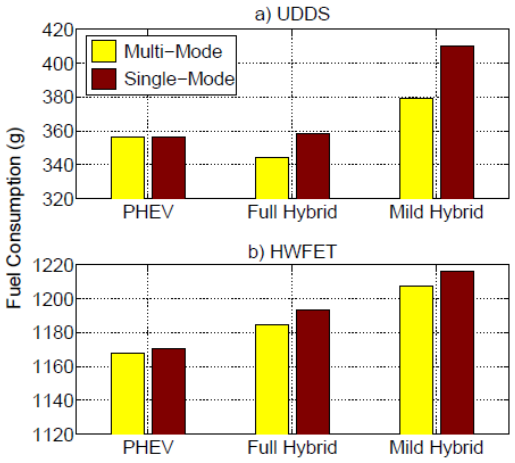

Figure 12: Fuel consumption for the multi-mode and single-mode engines in the parallel HEV architecture for two driving cycles and three electrification levels.

5. Conclusions

Here is the summary of the major findings from this work for the electrified multi-mode LTC-SI experimental setup studied in this paper:

• The improvement in fuel economy by converting a conventional SI engine-based HEV to an HEV with a multi-mode LTC-SI engine is significantly more in the series architecture, compared to the parallel architecture. Compared to full electrified vehicles

such as PHEVs, mild electrified vehicles such as mild HEVs are better suited to improve fuel economy in the multi-mode LTC-SI engine.

• The simulation results for the UDDS cycle show the single-mode HCCI and RCCI in series HEV offer up to 11.0% and 5.4% fuel consumption improvement, respectively over a single-mode SI in the series HEV platform. These improvements increase to 12.1% and 9.1% in the HWFET driving cycles for the HCCI and RCCI engines over the SI engine. This is due to longer engine ON time in the high-power-demand driving cycles. This provides more opportunity for the HCCI and RCCI engines to save more fuel compared to the SI engine.

• Integrating a multi-mode LTC in series HEV offers up to 1.4% more fuel consumption improvement compared to the best fuel consumption for the single-mode LTC engine in this study. This improvement depends on the type of driving cycle. Lower power-demand driving cycles show higher fuel economy improvement. The multi-mode LTC in series HEV has 12.4% fuel consumption reduction in the UDDS driving cycle, compared to the conventional SI mode.

• The results for the UDDS driving cycle show the multi-mode LTC-SI engine offers up to 7.5% fuel saving over a single-mode SI engine in the parallel HEV. This improvement reduces to 0.7% for the HWFET driving cycle. This is because, in the highway driving cycle, the high power at wheels happen at high vehicle speeds, so the optimal control strategy needs to locate the engine operating points in the best BSFC region of the SI mode and run for a shorter time compared to the mild hybrid.

6. Acknowledgements

This work was partially supported by the United States National Science Foundation under Grant No. 1434273. The authors would like to thank Dr. Mohammad Shakiba from Ford Motor Company for technical comments on analysis of PMP results. In addition, Dr. Seyfi Polat, Dr. Hamit Solmaz, Paul Dice, and Michigan Tech. Energy Mechatronis Laboratory (EML) graduate students are acknowledged for their contributions in building the experimental powertrain setup in this study.

7. References

[1] United States National Research Council, “Cost, Effectiveness, and Deployment of Fuel Economy Technologies for Light-Duty Vehicles”, Washington, DC: The National Academies Press, 2015,doi:10.17226/21744.

[2] European Commission Climate Action, https://ec.europa.eu/clima/policies. Accessed on Nov. 15, 2016.

[3] M. Berube. PHEVs - A Transition to the Future? SAE Range Extenders for Electric Vehicles Symposium, Knoxville, TN, USA, Nov. 2016.

[4] R. Sarkar. “Balancing Regulations and Customer Expectations in Future Powertrain, Fuel, Lubricant Vehicle Systems”. SAE International Powertrains, Fuels and Lubricants Meeting, Baltimore, USA, Oct. 2016.

[5] Z. Gao, S.J. Curran, J.E. Parks, D.E. Smith, R.M. Wagner, C.S. Daw, K.D. Edwards, and J.F. Thomas. “Drive Cycle Simulation of High Efficiency Combustions on Fuel Economy and Exhaust Properties in Light-Duty Vehicles”. Applied Energy, 157:762–776, 2015.

[6] T.V. Johnson. “Review of Diesel Emissions and Control”. Int. Journal of Engine Research, 10(5):275–285, 2009.

[7] M. Shahbakhti and C.R. Koch. “Characterizing the Cyclic Variability of Ignition Timing in a Homogeneous Charge Compression Ignition Engine Fuelled with n-heptane/iso-octane Blend Fuels”. International Journal of Engine Research, 9(5):361–397, 2008.

[8] S. Curran, Z. Gao, and R. Wagner. “Reactivity Controlled Compression Ignition Drive Cycle Emissions and Fuel Economy Estimations Using Vehicle Systems Simulations with E30 and ULSD”. SAE International Journal of Engines, 7:902–912, 2014.

[9] R. Reitz and G. Duraisamy. “Review of High Efficiency and Clean Reactivity Controlled Compression Ignition Combustion in Internal Combustion Engines”. Progress in Energy and Combustion Science, 46(4):12–71, 2015.

[10] M. Shahbakhti and C.R. Koch. “Physics-Based Control Oriented Model for HCCI Combustion Timing”. ASME Journal of Dynamic Systems, Measurement and Control, 132(2), 2010.

[11] M. Nazemi and M. Shahbakhti. “Modeling and Analysis of Fuel Injection Parameters for Combustion and Performance of an RCCI Engine”. Applied Energy, 165:135–150, 2016.

[12] J. Benajes, A. García, J. Monsalve-Serrano, I. Balloul, and G. Pradel. “An Assessment of the Dual-Mode Reactivity Controlled Compression Ignition/Conventional Diesel Combustion Capabilities in a EURO VI Medium-Duty Diesel Engine Fueled with an Intermediate Ethanol-Gasoline Blend and Biodiesel”. Energy Conversion and Management, 123:381–391, 2016.

[13] M. Fathi, O. Jahanian, and M. Shahbakhti. “Modeling and controller design architecture for cycle-by-cycle combustion control of homogeneous charge compression ignition (hcci) engines–a comprehensive review”. Energy Conversion and Management, 139:1–19, 2017.

[14] A. Solouk, M. Shakiba-herfeh, K. Kannan, H. Solmaz, P. Dice, M. Bidarvatan, N.N.T. Kondipati, and M. Shahbakhti. Fuel Economy Benefits of Integrating a Multi-Mode Low Temperature Combustion (LTC) Engine in a Series Extended Range Electric Powertrain. SAE Technical Paper No. 2016-01-2361, 2016.

[15] A. Solouk, M. Shakiba-herfeh, and M. Shahbakhti. Analysis and Control of a Torque Blended Hybrid Electric Powertrain with a Multi-Mode LTC-SI Engine. SAE Int. J. of Alternative Powertrains, 15 pages, 6(1):2017, doi:10.4271/2017-01-1153, 2017.

[16] M. Shahbakhti, A. Ghazimirsaied, and C.R. Koch. Experimental Study of Exhaust Temperature Variation in a Homogeneous Charge Compression Ignition Engine. Proceedings of the Institution of Mechanical Engineers, Part D: Journal of Automobile Engineering, 224(9):1177–1197, 2010.

[17] J.K. Arora. Design of Real-Time Combustion Feedback System and Experimental Study of an RCCI Engine for Control. MSc. Thesis, Michigan Technological University, 2016.